Characteristics of phosphate adsorption onto granulated coal ash in seawater

Satoshi Asaoka[a*], Tamiji Yamamoto[b*]

a) Graduate School of Biosphere Science, Hiroshima University

1-4-4 Kagamiyama, Higashi-Hiroshima, Japan 739-8528

Present: Graduate School of Science, Hiroshima University

1-3-1 Kagamiyama, Higashi-Hiroshima, Japan 739-8526

b) Graduate School of Biosphere Science, Hiroshima University

1-4-4 Kagamiyama, Higashi-Hiroshima, Japan 739-8528

*Corresponding author

Tel: +81-82-424-7945

Fax: +81-82-424-7998

E-mail address: st-asaoka@hiroshima-u.ac.jp

Graduate School of Science, Hiroshima University

1-3-1 Kagamiyama, Higashi-Hiroshima, Japan 739-8526

Abstract

Deterioration of sediments is one of the serious environmental problems. Controlling nutrient release flux from the sediments is important to alleviate eutrophication in addition to reducing terrigenous nutrient load. The purpose of this study is to evaluate phosphate removal performance of granulated coal ash (GCA) from seawater, which is produced from coal thermal electric power generation. Batch experiments were carried out to investigate removal kinetics of phosphate from seawater both under oxic and anoxic conditions. Phosphate was removed well from seawater both for oxic and anoxic conditions. Adsorption isotherm for phosphate revealed the GCA could remove phosphate effectively from seawater above the concentration of 1.7 μmol L^{-1}. GCA can reduce concentration of phosphate in seawater effectively under the anoxic conditions as such iron type adsorbents cannot be applied. Therefore, GCA can be a promising material to adsorb phosphate in the organically enriched sediment which is generally under highly reductive conditions.

Key words

adsorption, calcium phosphate, coal ash, eutrophication, phosphate, sediment

1. Introduction

Eutrophication is one of the most serious environmental problems affecting the quality and sustainability of enclosed water bodies worldwide, with the resultant bloom of primary producers presenting some deleterious effects down the food chain. Decomposition of dead phytoplankton cells accumulated in the bottom, for example, can lead to significant depletion of dissolved oxygen (DO) and causes a decrease in the oxidation reduction potential (ORP) of the sediments. The depletion of DO in the bottom layer of the water column is often harmful to the benthic ecosystem and its inhabitants and sometimes has negative impacts on the various aquaculture activities conducted there. On the other hand, the decrease in the ORP can trigger enhanced phosphate releasing fluxes from the sediment (Li et al., 1972; Krom and Berner, 1980) as well as the generation of toxic hydrogen sulfide by sulfate reduction (Rickard and Morse, 2005).

One of the well-documented causes of eutrophication is increased nutrient releasing flux from organically-enriched sediment in addition to terrigenous nutrient loading. An example can be seen in the Seto Inland Sea which is the largest semi-enclosed marine area in Japan with an area of 23,000 km^2 and an average depth of 38 m. In the entire Seto Inland Sea, the phosphate releasing flux from sediments ranged from 4.8 to 23.3 ton-P d^{-1} or 0.28 to 1.4 mg-P m^{-2} d^{-1}(Yamamoto et al., 1998). The phosphate releasing flux from sediment is one of the factors in eutrophication. . Therefore, it is important for alleviating eutrophication to reduce the phosphorus release flux from the sediments as well as to cut down terrigenous nutrient loads.

One of the technologies used to suppress phosphate release flux from coastal sediments is to cover the sediment with marine sands collected from other less polluted areas. However, dredging for marine sand has been

prohibited since March 2006 in order to preserve the benthic environment of the Seto Inland Sea. Steel making slag has been used as a substitute for natural sand (Yamada et al., 1987; Numata et al., 1999) . However, phosphate ion cannot be adsorbed onto the slag because the ζ potential of slag is negative in natural seawater with pH 8 (Oguz, 2004; Xue et al., 2009). Furthermore, adsorption of phosphate onto slag competes with hydroxyl ion on the adsorption sites under an alkaline condition such as that in seawater (Oguz, 2005). This is one reason why the application of slag to the sediment is not suitable for the remediation of organically-enriched sediment in terms of cutting down phosphate flux from the sediment.

Granulated coal ash (GCA) is a by-product from coal thermal power stations. In 2005, 11 Mt of coal ash was generated from coal thermal power stations and other industries in Japan (Japan Coal Energy Center, 2009). Coal ash is classified into two types; bottom ash generated in boiler bottoms and fly ash contained in gaseous waste. The latter comprises 85-95 % of the total coal ash production. The GCA used in this study is the product of mixing fly ash with cement. Generally, the GCA has been used thus far for road beds, construction material and coarse aggregates for concrete. Therefore, proposing new utilization strategy for by-product from coal thermal power stations are expected to contribute towards promoting recycling consciousness and waste reduction within the society.

GCA has been characterized and field tested for the remediation of degraded coastal environments. It was found that the GCA is composed of quartz and aluminosilicate and that environmentally regulated substances dissolved from the GCA were obviously below the maxima set as soil pollution environmental criteria in Japan (Asaoka et al., 2008). Most hazardous trace metals are not released from coal into seawater (Cabon et al.,

2007). The potential release of PAHs into seawater is not significant and their concentration is too low to be detectable (Jaffrennou et al., 2007). However, since their leaching process will depend on composition and physico-chemical properties of coal, it is essential for the sake of environmental safety to have their dissolution behavior checked before using phosphate absorbents.

A flow-through experimental system was also tested to simulate the semi-enclosed water bodies. The application of GCA decreased the concentration of PO_4^{3-} in the pore water effectively, and reduced phosphate releasing flux from the sediment into overlying water by 37-44% compared to the control (Asaoka et al., 2009). However, adsorption mechanisms remain to be solved.

Before eventually applying the GCA material to natural sediments in situ, it is important to evaluate its phosphate adsorption performance and mechanisms. Furthermore, it is important to correct parameters such as adsorption rate and adsorption capacity which will be required to design a simulation model that estimates appropriate and efficient application of GCA scientifically. This will help towards proposing an optimum strategy for the remediation of organically-enriched sediments in the future. This study also offers new insights into the possible reuse of otherwise worthless GCA, and this exciting information opens up many prospects for its application.

Thus, the purpose of the present study is to reveal the adsorption characteristics of phosphate onto GCA using batch experiments.

2. Materials and methods

2.1. Granulated coal ash (GCA)

The sediments used for remediation experiments consisted of fine grain such as mud/clay containing high amount of organic matters. However, the pulverized fly ash produced from coal thermal power station is very fine grained. Therefore, if the pulverized fly ash without granulation is mixed with the fine grain sediment, the sediment-pulverized fly ash mixtures will be muddier, which will not improve the sediment quality, but instead make it worse and less desirable for the experiments. On the other hand, the coarse grained GCA used in this study is a commercially-sold product named 'Hi-beads' (Energia Eco Materia Co., Inc.) with 5 mm diameter, which is produced through the granulation process of pulverized fly ash from coal firing systems generated from thermal power stations (Chugoku Electric Power Co. Inc.) by adding 15% cement as binder. The GCA is suitable for improving the sediment quality compared with fine grained pulverized fly ash.

The GCA used in the present study is mainly composed of SiO_2, CO_3, Al_2O_3 , CaO, C and Fe_2O_3 comprising quartz and aluminosilicate crystals, with their concentrations at 395, 133, 126, 55.4, 27.4 and 22.5 g kg^{-1}, respectively (Table1; (Asaoka et al., 2008)). The specific surface area is 21.1 m^2 g^{-1} (Asaoka et al., 2008).

2.2. Adsorption experiment

2.2.1. Removal kinetics

Phosphate solution was prepared as follows: tris-HCl buffer (Wako Pure Chemical Industries) was added to fiberglass (GF/C, Whatman) filtered seawater (salinity; 3.3%) collected from offshore of Ehime prefecture in Japan to constitute its final concentration to 30 mmol L^{-1}. Thereafter, aliquots of KH_2PO_4 (Kanto Chemical) were added to the seawater to make

the final concentration of 50 or 100 μmol L^{-1}, and 0.1 mol L^{-1} HCl was added to adjust pH to 8.2. The level of the phosphate concentration set above is assumed to be the concentration in the pore water of organically-enriched sediments in some inlets of Hiroshima Bay in Japan (Asaoka et al. 2009).

The experiment was carried out under both oxic and anoxic conditions. Under oxic conditions, 10 g of GCA was added to 1 L of seawater in a PTFE flask and capped with a PTFE membrane filter (45-430, Nalge Nunc International) to enable air exchange, and then stirred at a speed of 100 rpm at 22 °C. Under anoxic conditions, the same amount of GCA added seawater was prepared in a BOD bottle. The gas phase in the head of the bottle was replaced with N_2 gas and capped tightly and was stirred at a speed of 100 rpm at 22 °C. After 0-672 h incubation, the seawater was filtered through a hydrophilic PTFE membrane filter with a 0.45 μm pore (Millex, Millipore) and concentration of phosphate in the filtrates was determined by ascorbic acid reduction molybdate blue adsorption spectrophotometry (APHA, 1989) using an auto analyzer (SWATT, BLTEC). A blank test in the absence of GCA was also conducted following the same procedure to compensate for dissolved phosphate loss due to precipitation such as formation of calcium phosphate and magnesium phosphate and consumption by biological activities, etc. These experiments were conducted in triplicates.

2.2.2. Adsorption isotherm

Since the adsorption kinetics for phosphate adsorption onto GCA did not show significance between under the oxic and anoxic conditions, the adsorption test for isotherm was only conducted under oxic conditions. Phosphate solution with a concentration range of 0-300 μmol L^{-1} was

prepared following the same procedure described above. 50 mL of phosphate solution was dispensed into a 100 mL Erlenmeyer flask and 0.5 g of GCA was added to the solution. The flask was capped by a silicon plug to enable the flask to exchange air, and then it was stirred at 100 rpm at 22°C until achieving equilibrium (14-21 d) at which time phosphate concentration was measured by the same method as the removal kinetics analyses using an auto analyzer (SWATT, BLTEC). A blank test in the absence of GCA was also conducted following the same procedure to compensate for dissolved phosphate loss as described above. These experiments were conducted in triplicates.

2.3. X-ray diffraction of GCA

X-ray diffraction (XRD) pattern of the GCA was compared with and without adsorption of phosphate. The GCA sample with adsorption was prepared following the same procedure as the adsorption test for isotherm determination with initial phosphate concentration of 100 μmol L^{-1}. Prior to the XRD analyses, the sample was dried in an oven at 60 °C for 24 h, and ground using an agate mortar. Thereafter, XRD was recorded by a XRD instrument (RINT-1100K, Rigaku) using Cu Kα radiation at 34 kV, 14 mA.

3. Results and discussion

3.1 Removal kinetics

Change in phosphate concentration over time is shown in Fig. 1. The concentration of phosphate decreased and reached equilibrium in 336 h for initial concentration of 50 μmol L^{-1} and 504 h for 100 μmol L^{-1}, respectively, both under oxic and anoxic conditions. The concentrations at equilibria were 24 μmol L^{-1} for initial concentration of 50 μmol L^{-1} and 44-46 μmol L^{-1}

for 100 μmol L^{-1}, respectively. The adsorption kinetics (amount of adsorbed phosphate onto 1 g of GCA vs. contact time) were expressed as pseudo–first-order kinetic equation (Onganer and Temure, 1998), pseudo-second-order kinetic equation (Ho and McKay, 1999) and intra particle diffusion equation (Chang and Juang, 2004) as described by equations 1, 2 and 3, respectively.

$$\log(Q_e - Q_t) = \log Q_e - \frac{K_1}{2.303}t \qquad (1)$$

$$\frac{t}{Q_t} = \frac{1}{K_2 Q_e^2} + \frac{1}{Q_e}t \qquad (2)$$

$$Q_t = K_d t^{\frac{1}{2}} \qquad (3)$$

Where, K_1: pseudo-first-order rate constant (h^{-1}), K_2: pseudo-second-order rate constant (g μmol^{-1} h^{-1}), K_d: intra particle diffusion rate constant (μmol $h^{-1/2}$), Q_e: the amount of phosphate adsorbed onto GCA at equilibrium, (μmol g^{-1}), Q_t: the amount of phosphate adsorbed onto GCA at time t (μmol g^{-1}), t: contact time (h).

The correlation coefficient of each equation fitted to the experimental data is shown in Table 2. The pseudo-second-order kinetic equation described by equation (2) fitted well with the data under both oxic and anoxic conditions (Fig. 2), which suggested the phosphate adsorption was performed through two processes such as adsorption and precipitation of calcium phosphate.

The results under the oxic condition with initial phosphate concentration of 50 μmol L^{-1}, the pseudo-second-order kinetic rate constant and the concentration at equilibria were 2.8 x 10^{-2} g μmol^{-1} h^{-1} and 2.5 μmol g^{-1} ,

respectively. Under anoxic conditions, they were 1.9 x 10^{-2} g μmol^{-1} h^{-1} and 2.7 μmol g^{-1}, respectively. Under oxic conditions with initial phosphate concentration of 100 μmol L^{-1}, the pseudo-second-order kinetic rate constant and concentration at equilibria were 1.3 x 10^{-2} g μmol^{-1} h^{-1} and 5.4 μmol g^{-1}, respectively. Under anoxic conditions, they were 6.2 x 10^{-3} g μmol^{-1} h^{-1} and 6.2 μmol g^{-1}, respectively. The initial rate of adsorption (v_o: μmol g^{-1} h^{-1}) was calculated followed by equations 4 and 5, respectively.

$$Q_t = \frac{K_2 Q_e^2 t}{1 + K_2 Q_e t} \qquad (4)$$

$$v_0 = k_2 Q_e^2 \qquad (5)$$

Where, K_2: pseudo-second-order rate constant (g μmol^{-1} h^{-1}), Q_e: the phosphate adsorbed at equilibrium (μmol g^{-1}), t: contact time (h), v_o: initial rate of adsorption (μmol g^{-1} h^{-1}), respectively. Therefore, the initial rates of phosphate adsorption were 0.17 and 0.36 μmol g^{-1} h^{-1} for initial concentration 50 and 100 μmol L^{-1}, respectively under oxic conditions. The initial rates of phosphate adsorption were 0.14 and 0.24 μmol g^{-1} h^{-1} for initial concentration 50 and 100 μmol L^{-1}, respectively, under anoxic conditions. The adsorption parameters obtained in this study are shown in Table 3.

3.2 XRD pattern of GCA

The XRD patterns of GCA with and without phosphate adsorption are shown in Fig. 3. Four peaks (2θ : 14.7°, 20.7°, 21.7°, 23.8°) were observed for the GCA with adsorption. These peaks were identified as calcium

phosphate from comparisons with known standards (JCPDS, 1980). As shown in Table 1, calcium contents in the GCA was 55.4 g-CaO kg^{-1}. The calcium ion dissolution from GCA into seawater was observed and pH (H_2O) of GCA was 10.2 (Asaoka et al., 2008). It presents a suitable condition for the formation of calcium phosphate (Maclaren and Cameron, 1990). According to Maclaren, phosphate precipitates as aluminum phosphate and iron phosphate in acidic conditions, while at pH above 7 phosphate precipitates as calcium phosphate. Thus, the phosphate adsorbed onto GCA is determined to be calcium phosphate as corroborated in several papers (Yan et al., 2007; Pengthamkeerati et al., 2008). Iron phosphate (III) is dissolved when Fe (III) is reduced to Fe (II) under reduced conditions because the solubility of Fe (II) is much higher than that of Fe (III). Unlike phosphate adsorbed by iron, calcium phosphate does not dissolve under these reduced conditions. Therefore, the GCA is suitable for adsorbing phosphate in reduced conditions such as organically-enriched sediments accumulated in the bottom of enclosed water bodies.

3.3 Adsorption isotherm for phosphate onto GCA

The adsorption isotherm for phosphate onto GCA is shown in Fig. 4. The adsorption isotherm shows that phosphate was adsorbed onto GCA when its concentration is above 1.7 μmol L^{-1}. Above 1.7 μmol L^{-1} concentration the amount of phosphate is directly proportional to its initial concentration. These results suggest that the GCA can decrease the concentration of phosphate in the sediment pore water effectively because concentration of phosphate in organically enriched sediment was high, for example, it was higher than 40 μmol L^{-1} in the small inlet located at north end of Hiroshima Bay (Asaoka et al. 2009). However, GCA cannot be applied to adsorb

phosphate of overlying waters in terms of its low adsorption capacity in the lower concentration range, generally 0-2 μmol L^{-1} . The adsorption of phosphate cannot be expressed as general adsorption isotherms such as Langmuir plots, Freundlich plots and Henry plots because phosphate was adsorbed onto GCA by adsorption and accompanied by the formation of calcium phosphate.

Within the phosphate concentration range used in this study, the amount of adsorbed phosphate onto GCA was lower than that of fly ash (29-950 μmol g^{-1} (Yan et al., 2007)), steel making slag (170 μmol g^{-1} (Xiong et al., 2008), blast furnace slag (100-610 μmol g^{-1} (Kostura et al., 2005)) and aluminosilicate (530 μmol g^{-1} (Asaoka et al., 2006)). However, it was same as bottom ash (2.6-25 μmol g^{-1}; Yan et al., 2007). Although the amount of adsorbed phosphate onto GCA is low compared with other materials, GCA can reduce concentration of phosphate effectively under the anoxic conditions as such iron type adsorbents cannot be applied. Thus, GCA is more suitable than the other material for remediation of enclosed water bodies where the sediment condition was generally very reductive.

4. Conclusions

The purpose of the present study is to reveal adsorption characteristics of phosphate onto granulated coal ash (GCA) produced from coal thermal electrical power generation. The results were as follows:

(1) The adsorption kinetics of phosphate onto GCA was expressed as pseudo-second-order equation both under oxic and anoxic conditions, which suggested the phosphate adsorption was performed through two processes such as adsorption and precipitation of calcium phosphate.

(2) Adsorption isotherm for phosphate onto GCA revealed the GCA could

remove phosphate effectively from seawater above its initial concentration of 1.7 μmol L^{-1}. GCA was suitable for adsorbing phosphate in sediment pore water to cut down phosphate flux from organically-enriched sediment accumulated in the bottom of enclosed water bodies.

(3) XRD patterns of GCA showed phosphate was adsorbed onto granulated coal ash by the formation of calcium phosphate. Therefore, GCA can adsorb phosphate even under reduced conditions. Thus, GCA can reduce concentration of phosphate in seawater effectively under the anoxic conditions as such iron type adsorbents cannot be applied. Therefore, GCA was a promising material to adsorb phosphate in the organically enriched sediment which is generally under highly reductive conditions.

It is not difficult to provide enough amount of GCA for remediation of coastal sediments because some mass production plants for the materials are in operation. For example, according to one manifacturer, the maximum daily output of GCA is 600 t per plant represents an average production. For a further studies we are planning to apply GCA to organically enriched sediment in situ and monitoring remediation processes of the sediment, and subsequently, designing the simulation model by combining field data with the parameters collected in this study in order to propose an optimum application strategies such as amount of GCA application and frequency of treatment by estimating its remediation efficiency.

Acknowledgements

The authors would like to thank Chugoku Electric Power Co., Inc. and Energia Eco Materia Co., Inc. for kindly providing GCA for our study. The authors would also thank the financial support granted by the Graduate School of Biosphere Science, Hiroshima University. This manuscript has

been critically edited by a native English speaker Dr. Lawrence M. Liao of the Graduate School of Biosphere Science, Hiroshima University.

References

American Public Health Association, American Water Works Association, Water Pollution Control Federation, 1989. Standard method for examination of water and waste water. APHA, Washington DC, pp. 3000-4500.

Asaoka, S., Kawai, M., Aono, M., 2006. Adsorption characteristics of ammonium and phosphate in food industrial wastewater onto aluminosilicate. Jpn. J. of Soil Sci.and Plant Nutr. 778, 533-539. (in Japanese with English abstract).

Asaoka, S., Yamamoto, T., Yamamoto, K., 2008. A preliminary study of coastal sediment amendment with granulated coal ash -nutrient elution test and experiment on *Skeletonema costatum* growth-. Journal of Japan Society on Wat. Environ. 31, 455-462. (in Japanese with English abstract)

Asaoka, S., Yamamoto, T., Yoshioka, I., Tanaka, H., 2009. Remediation of coastal marine sediments using granulated coal ash. J. Hazard. Mater. 172, 92-98.

Cabon, J.Y., Burel, L., Jaffrennou, C., Giamarchi, P., Bautin F., 2007. Study of trace metal leaching from coals into seawater. Chemosphere 69, 1100-1110.

Chang, M.Y., Juang, R.S., 2004. Adsorption of tannic acid, humic acid, and dyes from water using the composite of chitosan and activated clay. J. Colloid Interf. Sci. 278., 18-25.

Ho, Y.S., McKay, G., 1999. Pseudo-second order model for sorption processes.

Process Biochem. 34, 451-465.

Jaffrennou, C., Stephan, L., Giamarchi, P., Cabon, J.Y., Burel-Deschamps, L., Bautin, F., 2007. Direct fluorescence monitoring of coal organic matter released in seawater. J. Fluoresc. 17, 564-572.

Japan Coal Energy Center. http : // www. jcoal. or. jp /coalash/ pdf/ CoalAsh_H18productiondata. (in Japanese), (accessed on 18 Feb. 2009).

JCPDS, 1980. Powder diffraction file. 21-839, USA, p. 269

Kostura, B., Kulveitová, H., Leško, J., 2005. Blast furnace slags as sorbents of phosphate from water solutions. Wat. Res. 39., 1795-1802.

Krom, M.D., Berner, R.A., 1980. Adsorption of phosphate in anoxic marine sediments. Limnol. Oceanogr. 25., 797-806.

Li, W.C., Armstrong, D.E. Williams, J.D. H., Harris, R.F., Syers, J.K., 1972. Rate and extent of inorganic phosphate exchange in lake sediments. Soil Sci. Soc. America J. 36, 279-285.

Maclaren, R.G., Cameron, K.C., 1990. Soil Science, Oxford University Press, UK, p.294.

Numata, N., Miyata, Y., Toyoda, Y., Sato, Y., Oda, S., 1999. Applicability of steel-making slag as improvement of bottom sediment (I). Bull. Soc.Sea Wat. Sci. Jpn. 53, 283-294. (in Japanese with English abstract)

Oguz. E., 2005. Thermodynamic and kinetic investigations of PO_4^{3-} adsorption on blast furnace slag. J. Colloid Interf. Sci. 281, 62-67.

Oguz, E., 2004. Removal of phosphate from aqueous solution with blast furnace slag. J. Hazard. Mater. 114, 131-137.

Onganer, Y., Temur, C., 1998. Adsorption dynamics of Fe(III) from aqueous solutions onto activated carbon. J. Colloid Interf. Sci. 205., 241-244.

Pengthamkeerati, P., Satapanajaru T., Chularuengoaksorn, P., 2008. Chemical modification of coal fly ash for the removal of phosphate from

aqueous solution. Fuel 87., 2469-2476.

Rickard, D., Morse, J.W., 2005. Acid volatile sulfide (AVS). Mar. Chem. 97, 141-197.

Xiong, J., He, Z., Mahmood, Q., Liu, D., Yang, X., Islam, E., 2008. Phosphate removal from solution using steel slag through magnetic separation. J. Hazard. Mater. 152, 211-215.

Xue, Y., Hou, H., Zhu, S., 2009. Characteristics and mechanisms of phosphate adsorption onto basic oxygen furnace slag. J. Hazard. Mater. 162, 973-980.

Yamada, H., Kayama, M., Saito, K., Hara, M., 1987. Suppression of phosphate liberation from sediment by using iron slag. Wat. Res. 21., 325-333.

Yamamoto, T., Matsuda, O., Hashimoto, T., Imose, H., Kitamura, T., 1998. Estimation of benthic fluxes of dissolved inorganic nitrogen and phosphorus from sediments of the Seto Inland Sea. J. Oceanogr. 7, 151-158. (in Japanese with English abstract).

Yan, J., Kirk, D.W., Jia, C.Q., Liu, X., 2007. Sorption of aqueous phosphorus onto bituminous and lignitous coal ashes. J. Hazard. Mater. 148 , 395-401.

Table1 Chemical composition of GCA

Major elements (g kg^{-1})		Trace elements (mg kg^{-1})			
SiO_2	395	Ba	397	Rb	28.8
CO_3	133	MnO	329	Co	28.6
Al_2O_3	126	Zr	298	Cr	27.2
CaO	55.4	N	200	Ga	20.6
C	27.4	V	111	Nb	34.4
Fe_2O_3	22.5	Zn	88.9	Sc	14.5
MgO	8.1	Ce	69.7	Th	12.7
K_2O	6.1	Cu	58.9	Hf	6.7
H	5.2	Y	52.6	W	5.2
TiO_2	5.7	Nd	34.4	U	4.2
Na_2O	2.5	La	34.2	Yb	3.9
P_2O_5	1.9	Pb	29.3	Cs	3.2
Sr	0.4	Ni	29.2		

Table 2 Correlation coefficient of each equation fitted to adsorption kinetics

	Oxic		Anoxic	
Initial concentration (μmol L^{-1})	50	100	50	100
Pseud first order equation	0.958	0.945	0.963	0.972
Pseud second order equation	0.999	0.999	0.998	0.995
Intra particle diffusion equation	0.920	0.922	0.888	0.934

Table 3 Parameter concering phosphate adsorption onto GCA obtained in the present study

Paramaters	Oxic		Anoxic	
	50 μmol L^{-1}	100 μmol L^{-1}	50 μmol L^{-1}	100 μmol L^{-1}
Pseudo second order kinetic constant (g μmol^{-1} h^{-1})	2.8 X 10^{-2}	1.3 X 10^{-2}	1.9 X 10^{-2}	6.2 X 10^{-3}
Amount of phosphate adsorbed at equilibulium (μmol g^{-1})	2.5	5.4	2.7	6.2
Initial rate (μmol g^{-1} h^{-1})	0.17	0.36	0.14	0.24

Fig. 1 Time change in phosphate concentrations with initial concentrations of 50 μmol L^{-1} oxic (□), 100 μmol L^{-1} oxic (○), 50 μmol L^{-1} anoxic (■) and 100 μmol L^{-1} anoxic (●). The 10 g L^{-1} of GCA was added to the seawater at pH 8.2 under oxic or anoxic condition and stirred for 672 h at 22 °C. The error bars are standard deviations conducted in triplicates.

Fig. 2 Pseudo-second-order kinetics for the phosphate adsorption onto granulated coal ash with initial concentration: 50 μmol L^{-1} oxic (□) , anoxic (■), 100 μmol L^{-1} oxic (○) , anoxic (●).

Fig. 3 XRD patterns of PO_4^{3-} adsorbed onto GCA; ▽: calcium phosphate

Fig. 4 Adsorption isotherm for phosphate onto GCA. The error bars are standard deviations conducted in triplicates.

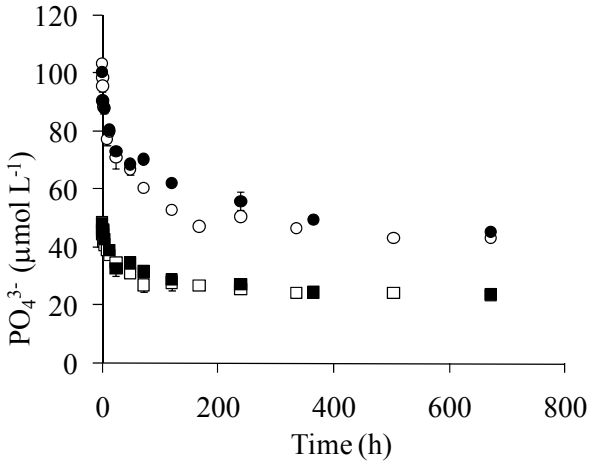

Fig. 1

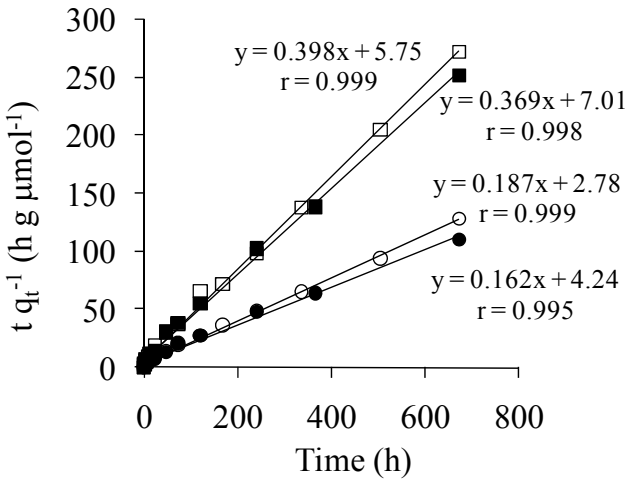
y = 0.398x + 5.75
r = 0.999
y = 0.369x + 7.01
r = 0.998
y = 0.187x + 2.78
r = 0.999
y = 0.162x + 4.24
r = 0.995
t q_t^{-1} (h g µmol^{-1})
Time (h)
0
50
100
150
200
250
300
0
200
400
600
800

Fig. 2

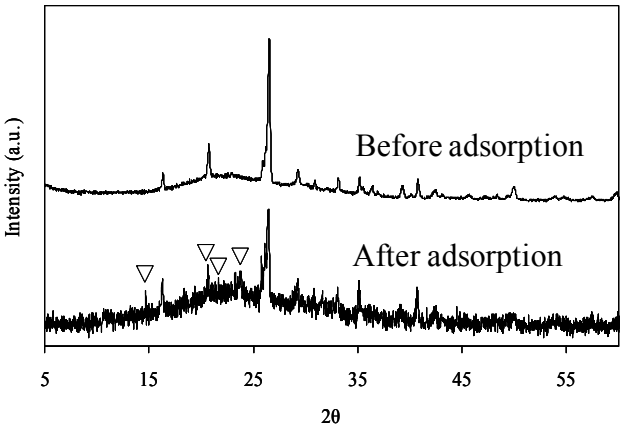
Intensity (a.u.)
Before adsorption
After adsorption
5
15
25
35
45
55
2θ

Fig. 3

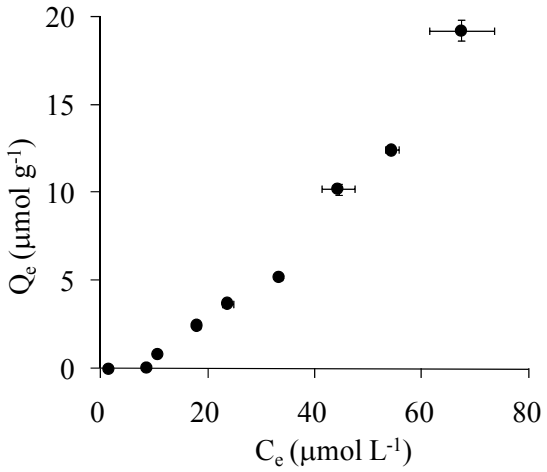

Fig. 4